The MCD and EPR of the Heme Centers of Nitric Oxide Reductase from *Pseudomonas stutzeri*: Evidence That the Enzyme Is Structurally Related to the Heme-Copper Oxidases†

Myles R. Cheesman,*,‡ Walter G. Zumft,§ and Andrew J. Thomson‡

Centre for Metalloprotein Spectroscopy and Biology, School of Chemical Sciences, University of East Anglia, Norwich NR4 7TJ, U.K., and Lehrstuhl für Mikrobiologie, Universität Fridericiana, D-76128 Karlsruhe, Germany

Received October 1, 1997; Revised Manuscript Received January 12, 1998

ABSTRACT: EPR spectra at liquid helium temperatures and MCD spectra at room temperature and 4.2 K are presented for fully oxidized nitric oxide reductase (NOR) from *Pseudomonas stutzeri*. The MCD spectra show that the enzyme contains three heme groups at equivalent concentrations but distinctive in their axial coordination. Two, in the low-spin ferric state at all temperatures, give rise to infrared charge-transfer transitions which show the hemes to have bis-histidine and histidine−methionine ligation, respectively. The EPR spectra show them to be magnetically isolated. The third heme has an unusual temperature-dependent spin state and spectroscopic features which are consistent with histidine−hydroxide coordination. No EPR signals have been detected from this heme. Together with its unusual near-infrared MCD, this suggests a spin−spin interaction between this heme and another paramagnet. The three hemes account for only 75% of the iron content, and it is concluded that the additional paramagnet is a mononuclear ferric ion. These results provide further evidence that NOR is indeed structurally related to heme-copper oxidases and that it contains a heme/non-heme iron spin-coupled pair at the active site.

In bacterial denitrification, nitrate is reduced to dinitrogen in four separate steps: $NO_3^- \rightarrow NO_2^- \rightarrow NO \rightarrow N_2O \rightarrow N_2$. The first of these reactions occurs at the inner face of the cytoplasmic membrane producing nitrite ion which is then exported to the periplasm where the three subsequent reduction steps take place (*1*−*4*). Of the four enzyme systems mediating these reactions, the last to be identified and the least well characterized is nitric oxide reductase (NOR)[1] (EC 1.7.99.7), a membrane-bound cytochrome *bc* complex which catalyzes the one-electron reduction of nitric oxide to N_2O (*5*−*8*). There was initially some doubt as to whether nitric oxide is a genuine free intermediate of denitrification (*9*−*11*). The alternative, that N_2O is produced directly from NO_2^- by a single enzyme, was ruled out when mutational inactivation of nitrite reductase yielded cultures which could still reduce NO (*12, 13*). A cytochrome *bc* complex with NO reductase activity was subsequently isolated from both *Pseudomonas stutzeri* and *Paracoccus denitrificans* (*5, 6*). Also a Nor$^-$ mutant of *P. stutzeri* possessing cytochrome cd_1 yielded NO as the product of NO_2^- reduction with little N_2O (*14*).

The enzyme from *P. stutzeri* was the first NOR to be isolated and was shown to be a heterodimeric complex with subunit masses of 53 kDa (NorB) and 17 kDa (NorC). The *b*-type heme is associated with NorB and the *c*-type with NorC (*5, 8, 15*). It was reported that the NorBC complex contains approximately two heme groups, and an EPR study identified both high- and low-spin ferric heme in approximately equal concentrations (*5*). The high-spin ferric heme EPR features represented three different species amounting to 0.75−0.85 heme per enzyme molecule. Two low-spin ferric heme species were detected at concentrations of 0.96 and 0.1−0.3 spin per molecule, respectively (*15*). In contrast, the NOR from *P. denitrificans* was reported to contain *b*- and *c*-type hemes in a 2:1 ratio (*16*).

The primary structure of the *P. stutzeri* NOR shows little homology with any other known protein sequences although hydropathy analysis suggested that NorB forms 12 membrane spanning segments with potential histidine heme ligands close to the periplasmic face of the membrane (*1, 17*). However, subsequent examination indicated sequence similarities between NOR and two of the subunits of the cbb_3-type of cytochrome *c* oxidases. Thus it was suggested that there is a significant structural similarity between bacterial NOR and the heme-copper oxidases (HCOs) (*18, 19*). The determination of the *norB* sequences of the enzymes from *Pseudomonas aeruginosa* (*20*) and *P. denitrificans* (*21*) lent further support to this proposal.

The HCOs constitute a super-family of terminal oxidases, which catalyze the four-electron reduction of dioxygen to

† This work was supported by BBSRC Grant BO3032-1 (A.J.T.) and by the Deutsche Forschungsgemeinschaft and Fonds der Chemischen Industrie (W.G.Z.).

* Author to whom correspondence should be addressed at the School of Chemical Sciences, University of East Anglia, Norwich NR4 7TJ, United Kingdom. Telephone: +44 (1603) 592028. Fax: +44 (1603) 592710. E-mail: m.cheesman@uea.ac.uk.

‡ University of East Anglia.

§ Universität Fridericiana.

[1] Abbreviations: NOR, nitric oxide reductase; HCO, heme-copper oxidase; CCO, cytochrome *c* oxidase; *P. stutzeri*, *Pseudomonas stutzeri*; *P. denitrificans*, *Paracoccus denitrificans*; *P. aeruginosa*, *Pseudomonas aeruginosa*; EPR, electron paramagnetic resonance; MCD, magnetic circular dichroism; NIR-CT, near-infrared charge transfer; RT, room temperature.

S0006-2960(97)02437-9 CCC: $15.00
Published on Web 02/24/1998

water and couple the free energy to the creation of a transmembrane proton gradient. They exhibit variable composition but all contain a common core of three subunits which exhibit high levels of sequence homology (*18, 22*). Three-dimensional structures have been determined for two of these oxidases, cytochrome aa_3 from *P. denitrificans* (*23*) and cytochrome *c* oxidase (CCO) from bovine cardiac muscle (*24, 25*). These confirm earlier conclusions, based on sequence and mutagenesis studies, that the large HCO subunit I comprises 12 membrane spanning helixes (*22*). Six invariant histidines act as ligands to the metal centers which are bound, in the case of the bacterial enzymes, close to the periplasmic side of the membrane. The active site contains one high-spin ferric heme in magnetic interaction with a cupric ion, known as Cu_B (*26*−*29*). Four of the conserved histidines act as ligands within this dinuclear site, one to the high-spin heme and three to Cu_B. The remaining pair of invariant histidines are the two axial ligands to a magnetically isolated low-spin ferric heme. The structural data are yet of insufficient resolution to identify with certainty what, if anything, lies within the active site directly between the two metal ions. This is an unresolved question for HCOs. Active site heterogeneity caused by variations in both oxidation and ligation state is a long-studied problem (*30*).

Analyses of NOR sequences show that NorB has 15−20% homology with subunit I of heme-copper oxidases and suggest that it also forms 12 membrane-spanning helixes (*17, 18, 20*). Furthermore, six of the histidine residues in NorB occur at positions analogous to those of the six totally conserved metal binding histidines of HCO subunit I. Thus, the postulated relationship between NOR and heme-copper oxidases requires the presence of two hemes within NorB, one possibly as part of a dinuclear site and one as a bis-histidine liganded low-spin heme. Subunit II of the HCOs varies in its prosthetic group content. In the quinol oxidases, it contains no metals (*31*). When soluble cytochrome *c* acts as electron donor then subunit II contains one of two types of metal center: the dinuclear copper site, Cu_A, in the case of CCO (*18*) and a *c*-type cytochrome in FixO, the equivalent subunit of cytochrome cbb_3-type oxidases (*32*−*35*). Both NorC and FixO contain a *c*-type heme binding motif and are predicted to comprise a globular region extending into the periplasm with an N-terminal membrane anchoring domain. Significantly, perhaps, cytochrome cbb_3 is the heme-copper oxidase whose sequence is the most similar to that of NOR (*18, 19, 32, 36*).

However, an important difference between HCOs and NOR is that elemental analysis of NOR preparations shows the absence of copper but a higher iron content than can be attributed to heme (*5, 17, 37, 38*). This has led to speculation that the HCO Cu_B site is replaced, in NOR, by some form of non-heme-iron site. Iron analyses of *P. denitrificans* NOR suggest a mononuclear site (*37*). The possibility that heme-copper oxidases are derived from an NOR structure in a modification which involves replacement of iron with copper at the active site is intriguing since it has long been known that CCO can reduce NO to N_2O but at rates several orders of magnitude lower than for NOR (*5, 15, 16, 38*−*41*). NOR from *P. denitrificans* (ATCC 35512) is reported to be able to reduce dioxygen (*16*).

We present here the results of a study of the oxidized state of *P. stutzeri* NOR using EPR and MCD spectroscopy which show that *P. stutzeri* NOR does indeed contain three distinct types of heme group at equivalent levels and that they correspond in terms of spin-state and coordination properties to those found in heme-copper oxidases, specifically the cytochrome cbb_3 enzymes.

MATERIALS AND METHODS

Enzyme Preparation. NOR was prepared from *P. stutzeri* ZoBell strain, ATCC 14405, purified to homogeneity, and analyzed for cofactors as previously described (*5, 15*). Samples for spectroscopic examination were prepared in deuterium oxide solutions containing 20 mM HEPES−NaOH, 0.5% dodecyl maltoside, and 0.3 M potassium chloride at pH* = 8.2 (pH* is the apparent pH of the D_2O solutions measured using a standard glass pH electrode). Spectra are plotted using a concentration value which is equal to 0.25 of the total iron content of the protein samples. Protein determinations by a modified Lowry method (*42*) give apparent concentrations ∼20% higher than this value but which are in disagreement with heme concentrations derived from the spectroscopic results presented below.

Spectroscopic Measurements. Electronic absorption spectra were recorded on a Hitachi U4001 spectrophotometer. EPR spectra were recorded on an X-band ER-200D spectrometer (Brüker Spectrospin) interfaced to an ESP1600 computer and fitted with a liquid helium flow-cryostat (ESR-9; Oxford Instruments). Magnetic circular dichroism (MCD) spectra were recorded on either a circular dichrograph, JASCO J-500D, for the wavelength range 280−1000 nm or a laboratory-built dichrograph (*43*) for the range 800−2500 nm using an Oxford Instruments SM4 split-coil superconducting solenoid capable of generating magnetic fields up to 5 T. To obtain optical quality glasses on freezing for low-temperature MCD measurements, glycerol was added to samples to a level of 50% v/v (*44*). These additions did not significantly alter the EPR or room-temperature electronic absorption spectra. Quantitation of low-spin ferric EPR signals was achieved by the method of Aasa and Vänngård (*45*) using 1 mM Cu(II)EDTA as a spin standard.

RESULTS

Electronic Absorption and MCD of Oxidized NOR at Room Temperature. Figure 1a shows the room-temperature absorption spectrum of oxidized NOR. The Soret band, at 412 nm, has an intensity of 312 mM^{-1} cm^{-1}, suggesting the presence of approximately three hemes (*46*). The spectrum includes no features clearly associated with high-spin ferric heme. There is, however, some very weak intensity between 640 and 740 nm which is characteristic of low-spin ferric hemes possessing at least one of the sulfur ligands methionine or cysteine. Cytochromes *c* (histidine−methionine), bacterioferritin (bis-methionine), and cytochrome P450 (cysteine−H_2O) all give rise to such absorption intensity (*47*−*49*).

Bands in the MCD spectrum to the high-energy side of 600 nm are due to $\pi-\pi^*$ transitions of the porphyrin macrocycle and are sufficiently sensitive to the properties of the iron so as to be diagnostic of its spin and oxidation state and can also provide a measure of heme concentration (*50*). At longer wavelengths, charge-transfer (CT) bands, involving porphyrin (π) → ferric (d) transitions, can be detected in the MCD spectrum: two for high-spin ferric heme

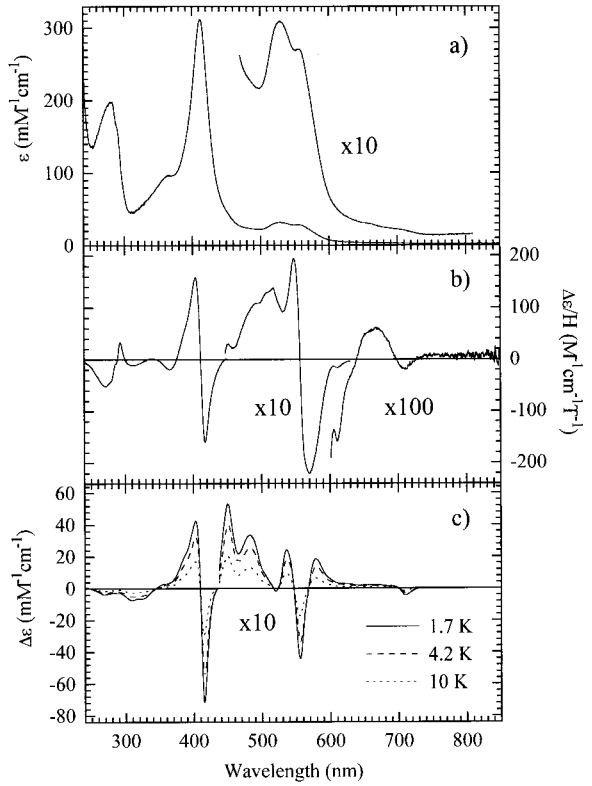

FIGURE 1: UV−visible spectra of *P. stutzeri* nitric oxide reductase. Buffers were as described in Materials and Methods. (a) Room-temperature electronic absorption spectrum. Sample concentrations used were 32 and 225 μM. (b) Room-temperature MCD spectrum. Sample concentrations used were 32 and 225 μM. The spectrum was recorded using a magnetic field of 6 T. (c) Low-temperature MCD spectra. Sample concentrations used were 18 and 95 μM. The spectra were recorded using a magnetic field of 5 T. Temperatures were 1.7 K (—), 4.2 K (- - -), and 10 K (•••).

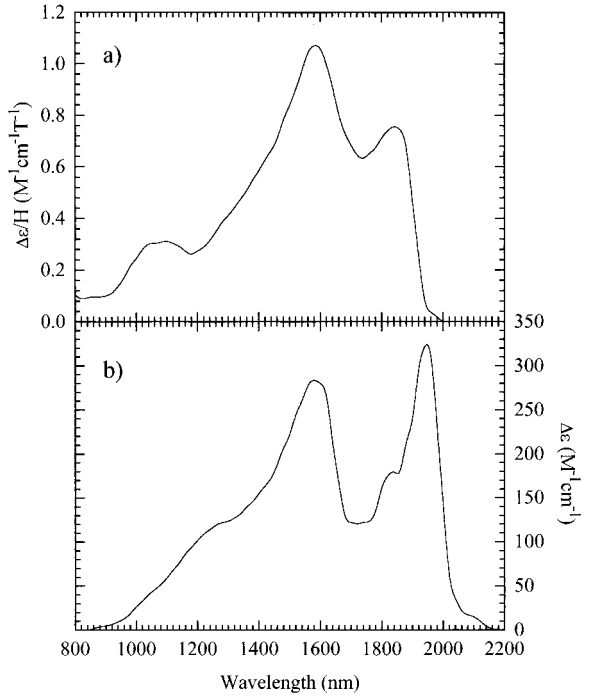

FIGURE 2: Near-infrared (NIR) MCD spectra of *P. stutzeri* nitric oxide reductase. Buffers were as described in Materials and Methods. (a) Room temperature spectrum. Sample concentration was 225 μM. The spectrum was recorded using a magnetic field of 6 T. (b) Spectrum at 4.2 K. Sample concentration was 95 μM. The spectrum was recorded using a magnetic field of 5 T.

and one for low-spin (*51*−*53*). The energy of the low-spin ferric heme CT transition is shifted by changes in heme coordination, and locating this band by MCD is a well-established method of identifying axial ligands (*43*, *50*). The positions of the high-spin CT transitions are also sensitive to the nature of the axial ligands but have been less extensively studied.

The UV−visible room-temperature MCD spectrum of oxidized NOR, Figure 1b, contains a derivative shaped band at the wavelength of the Soret absorption that is characteristic of low-spin ferric heme. At these energies, the low-spin ferric heme dominates the contribution from any high-spin heme. The peak-to-trough intensity provides a reliable measure of the number of low-spin hemes contributing. Since a value of $\Delta\epsilon = 150-160$ M^{-1} cm^{-1} T^{-1} is typical for one heme (*50*), the Soret region of Figure 1b is due to two low-spin ferric hemes. In the α-region, the intensity of the derivative shaped band with extrema at 548 and 570 nm is also typical for two low-spin ferric hemes. The sharp negative feature at 611 nm is assigned to a high-spin ferric heme. The intensity approximately -1 M^{-1} cm^{-1} T^{-1} is comparable to that observed for high-spin ferric heme o_3 in several derivatives of cytochrome bo_3 (*53*, *54*), but because of the presence of contributions from the other hemes, it is impossible to detect in the absorption spectrum. This wavelength is unusually blue-shifted for a high-spin ferric heme. A derivative shaped MCD band is clearly seen between 640 and 740 nm. This corresponds to the absorption intensity which was assigned to one thioether liganded heme.

In the room-temperature NIR MCD spectrum of oxidized NOR, Figure 2a, two CT bands are observed with maxima at 1585 and 1840 nm, wavelengths characteristic of bis-histidine and histidine−methionine ligation, respectively (*43*, *50*). The intensities of these peaks indicate that the two hemes are present at approximately equimolar levels.

In summary, the room temperature absorption and MCD spectra clearly indicate three distinct heme species, present at comparable levels. This conclusion is confirmed by the MCD spectra at low temperature in the near-infrared region (see later). Two of these hemes are low-spin ferric at room temperature with bis-histidine and histidine−methionine coordination, respectively. The third heme is high-spin with a CT band shifted to an unusually short wavelength.

EPR of Oxidized NOR at Low Temperature. The X-band EPR spectrum at 10 K, Figure 3, shows three features at $g = 2.97$, 2.25, ∼1.4 typical of a low-spin ferric heme coordinated by two histidine residues with approximately parallel ligand plane orientations (*55*). We therefore assign these signals to the bis-histidine coordinated heme detected in the room-temperature MCD spectra. Integration of the $g = 2.97$ feature using the method of Aasa and Vänngård (*45*) yields a concentration of ∼0.96 spin per mole of protein, consistent with the conclusion from the NIR MCD that bis-histidine heme accounts for one low-spin heme at room temperature.

Features near $g = 6$ and $g = 2$ represent minor amounts of high-spin ferric heme and small amounts of Cu(II), respectively. These small quantities represent no more than a few percent in terms of enzyme concentrations. Importantly, therefore the $g = 6$ signal cannot be correlated with

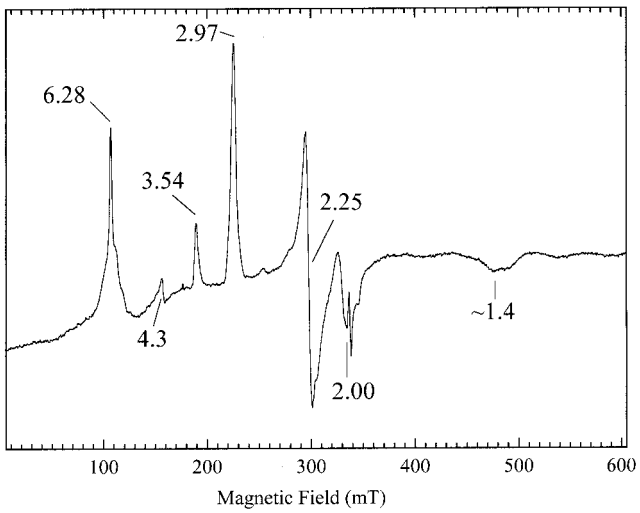

FIGURE 3: X-band EPR spectrum of oxidized *P. stutzeri* nitric oxide reductase. Buffers used were as described in Materials and Methods. The spectrum was recorded at 10 K using 1 mT modulation amplitude and 2.01 mW microwave power. The *g*-values of features discussed in the text are indicated.

any of the heme species already identified in the MCD spectra. Note that the signal at $g = 4.3$ which typically arises from a magnetically isolated non-heme iron center is also low in amplitude.

The feature at $g = 3.54$ is assigned as the g_z feature of the spectrum of a low-spin heme with histidine−methionine ligands. This high *g*-value together with the asymmetric or ramp shape of the signal shows that it is one component of a rhombic trio in which two of the *g*-factors are below 2. This leads overall to a broad "large g_{max}" type EPR spectrum where the other two *g*-values are not easily detected in the derivative mode (*55*). Consequently, quantitation of this species by EPR spin integration is less straightforward. Griffith showed that, in the limit of negligible covalency, the sum of the squares of the *g*-values of a low-spin ferric heme equals 16 (*56*). Assuming this to be the case, it can be shown that for large g_{max} species, where $g_z > 3.5$, uncertainty in the values of g_x and g_y yields an error in determination of the spin concentration of <1% (*57*). Using this approach, it was shown that the $g = 3.54$ feature in the EPR spectrum of *P. denitrificans* NOR represents 0.71 electron spin compared to 1 for the $g = 2.99$ signal (*37*). In the *P. stutzeri* NOR EPR spectrum of Figure 3, the ratio of amplitudes $g = 3.54/g = 2.97$ is higher than observed for *P. denitrificans*, and the same method of integration shows that the $g = 3.54$ signal also represents ~1 spin per mole of protein. This is consistent with the conclusions drawn from the MCD properties. The EPR properties are unaffected by the addition of 50% glycerol as a glassing agent for the optical studies.

MCD of Oxidized NOR at Low Temperature. In Figure 1c are the low-temperature UV−visible MCD spectra of oxidized NOR. These are dominated by the low-spin ferric heme, and the spectrum therefore gives an excellent measure of heme concentration. Since at 4.2 K a low-spin ferric heme typically yields a derivative Soret feature with a peak-to-trough intensity of ~32 mM^{-1} cm^{-1} (*50*), the value of 95 mM^{-1} cm^{-1} for NOR suggests *three* rather than two low-spin ferric hemes. The 611 nm trough seen at room temperature is no longer observed in the 4.2 K MCD.

This suggests that one heme of NOR has changed from high-spin at room temperature to low-spin ferric at 4.2 K. This is confirmed by examination of the NIR MCD which reveals a new low-spin CT band, Figure 2b. The NIR CT bands at 1585 and 1840 nm from the bis-histidine and histidine−methionine hemes, respectively, remain, but an additional positive MCD band is observed at 1945 nm. This is an unusual wavelength for the CT band of an isolated low-spin ferric heme. The typical wavelength ranges observed are 1740−1900 nm for histidine−methionine and 2140−2270 nm for methionine−methionine ligation. We therefore assign this peak to the third heme and postulate that its spin-state has undergone a temperature-dependent change from high-spin at room temperature to low-spin at 4.2 K. However, this additional low-spin Fe(III) heme is not apparent in the EPR spectrum. This suggests that it may be spin-coupled to another paramagnetic center.

DISCUSSION

The EPR Detectable Low-Spin Ferric Hemes. The MCD clearly shows the presence of two ferric hemes which are low-spin at all temperatures and have histidine−histidine and histidine−methionine ligation, respectively. These correspond to the two low-spin ferric hemes observed in the EPR spectrum. The latter is responsible for the absorption and MCD intensities in the 640−740 nm region. These and other spectral assignments are listed in Table 1.

NorB is the *b*-heme containing subunit structurally homologous to HCO subunit I which always contains a heme coordinated by two histidine residues orientated with parallel ligand planes, an arrangement characterized by a rhombic EPR spectrum with *g*-values close to the set of $g = 2.97$, 2.25, ~1.4 observed here. We therefore assign this set of *g*-values to the *b*-heme of NorB and not to the *c*-heme of NorC as has been suggested for *P. denitrificans* NOR (*37*).

The EPR signal with $g_z = 3.54$ is assigned to a histidine−methionine coordinated heme in NorC. This type of spectrum is typically observed for hemes with two perpendicularly orientated histidine ligands but can also arise in cases with histidine−methionine ligation, for example the $g = 3.64$ signal of cytochrome c_4 from *Azotobacter vinelandii* (*58*). The two reported EPR spectra of cytochromes cbb_3 also contain a large g_{max} type g_z feature from the heme *c* (*36, 59*), suggesting that the strong structural similarities between NOR and HCOs extend to subunit II.

Assignment of the 1585 nm MCD band to the species responsible for the $g = 2.97$, 2.25, ~1.4 EPR spectrum and the 1840 nm band to the $g_z = 3.58$ species relies on the NorB structural model and the invariant EPR spectra observed for the low-spin hemes of HCOs. There is however confirmation of these assignments in the NIR MCD spectra where ligand orientation governs the intensity of the MCD NIR CT band, especially in the low-temperature spectrum. For a specific ligand pair, the orientation which gives rise to a large g_{max} EPR spectrum also results in higher NIR MCD intensity. The 1585 nm band is undoubtedly due to a heme with bis-histidine ligation, but has too weak an intensity to have perpendicular ligand planes and so cannot correlate with the large g_{max} EPR spectrum.

The Active Site Heme. The room-temperature absorption spectrum of the heme-copper oxidase, cytochrome bo_3,

Table 1: Spin State and Axial Ligand Assignments of the Ferric Hemes of *P. stutzeri* NOR

		MCD spectra		EPR spectra	heme spin state	heme axial ligation
heme 1	RT[a]	intense bands 300−600 nm	positive band at 1585 nm		low-spin	histidine−histidine
	LT[b]	intense bands 300−600 nm	positive band at 1585 nm	$g = 2.97, 2.25, \sim 1.4$	low-spin	histidine−histidine
heme 2	RT	not detected 300−600 nm negative trough at 611 nm	derivative centered at ∼1100 nm		high-spin	histidine−hydroxide
	LT	intense bands 300−600 nm	positive band at 1945 nm	EPR silent	low-spin	histidine−hydroxide
heme 3	RT	intense bands 300−600 nm weak bands 640−740 nm	positive band at 1840 nm		low-spin	histidine−methionine
	LT	intense bands 300−600 nm weak bands 640−740 nm	positive band at 1840 nm	$g = 3.54, -, -$	low-spin	histidine−methionine

[a] Room temperature. [b] Low temperature: 10 K for EPR spectra and 4.2 K for MCD spectra.

contains a distinct shoulder at 625 nm which signifies the presence of high-spin ferric heme, in this case the heme o_3 at the dinuclear active site (*60*). This band normally appears in the MCD spectrum as a derivative shaped feature (*61*). In the presence of low-spin heme, which gives rise to intense signals at shorter wavelengths, the low-energy trough of this band is often the only isolated high-spin feature. A second derivative shaped high-spin CT MCD band also occurs at lower energies, typically 800−1300 nm. We have previously noted systematic shifts in the energies of both bands in response to axial ligand changes at high-spin heme o_3 of cytochrome bo_3 (*53*). For the higher energy CT band, MCD data are available for eight different ligand pairs (see refs *53* and *62* and references therein). These data are being extended by use of heme-pocket mutants of myoglobin, and we have characterized two novel histidine−tyrosinate liganded heme species (H. Seward, M. R. Cheesman, and A. J. Thomson, unpublished data). These and the majority of the data available for high-spin ferric hemes have histidine as one of the ligands. In the case of a histidine proximal ligand, a distinct pattern in the positions of the CT bands is clear, e.g., for histidine−H_2O ligation the two CT bands cluster around 640 and 1080 nm. If the iron is five−coordinate, the bands are red-shifted to positions near 660 and 1240 nm. For distal ligation by the anions fluoride, tyrosinate, or hydroxide the CT bands are blue-shifted to the regions 610−625 and 800−880 nm, respectively. The first CT band for the high-spin heme in NOR at room temperature is clearly visible at 611 nm which is consistent with histidine−X^- ligation to this heme, where X^- is an anion.

Although the intensities of the MCD bands of high- and low-spin ferric hemes at room temperature are comparable, at liquid helium temperatures there is a large difference, the intensity of the low-spin ferric heme MCD being a factor of 50−150 times greater than that of high-spin ferric heme (*50*). However, high-spin ferric heme gives rise to bands of relatively narrow width and can therefore be detected even when overlapped by the more intense transitions of low-spin ferric hemes. For example, the weak high-spin heme *o* MCD feature near 625 nm in the MCD of cytochrome bo_3 is still detectable against the background of low-spin heme bands (*60*) as is the feature at 614 nm for the fluoride derivative of cytochrome bo_3 (M. R. Cheesman, and A. J. Thomson, unpublished data). However, in the 4.2 K MCD spectrum of NOR, there is no trace of the 611 nm high-spin ferric feature and the low-spin MCD intensity has increased by ∼50%. This shows that a third low-spin ferric heme is contributing at 4.2 K to the MCD spectrum. Hence, this heme must have undergone a spin-state switch from high-spin to low-spin on cooling. We note that a thermal equilibrium between a low-spin ground state and a high-spin excited state would give at high temperatures equal mixtures of the two spin-states, whereas at low temperatures only one species would be expected to dominate the spectrum. However, in this case, the heme switched from 100% high- to 100% low-spin on cooling.

An important question remains concerning the nature of the ligands to the heme in the dinuclear site. The wavelength of the third low-spin NIR CT band is 1945 nm, a position between those regions associated with histidine−methionine and bis-methionine coordination. The energy of the CT band of low-spin Fe(III) hemes depends on the ligand field strength of the axial ligand(s). The field strength of a particular ligand can be modified by the protein environment in a number of ways; for example, an axial ligand may be constrained by steric effects to adopt an unusual orientation, by H-bonding to reduce the field strength, or by the presence of another ligating metal ion, such as Cu_B(II) in the dinuclear site of CCO and quinol oxidases. In the last case, the effect of a distal coordinating metal ion will be most pronounced if a ligand, X, bridges between the heme Fe(III) and the distal metal ion. For CCO and cytochrome bo_3, a NIR CT band is observed at anomalously long wavelengths when the active site heme is sent low-spin by binding of cyanide. Bridging to Cu_B mediates a spin−spin coupling between the two metals and also reduces the effective ligand strength of the cyanide ion at the iron. The band is consequently shifted from the position expected for histidine−cyanide liganded heme (∼1600 nm) to ∼1950 and 2050 nm, respectively (*53*, *63*).

The heme of the dinuclear site of NOR provides a clue to its ligand environment by its unusual spin-state temperature dependence. We have observed this behavior only in one other system, namely, the high-pH form of myoglobin. Previously accepted models of this species view it as a histidine−hydroxide liganded ferric heme in a thermal spin equilibrium between a low-spin ferric ground state and an excited high-spin state (*64*). However, we have recently reexamined hydroxymyoglobin and have observed, in the MCD properties, a high-spin heme with an MCD CT band minimum at 618 nm at room temperature which changes to a low-spin species at liquid helium temperatures (H. Seward, M. R. Cheesman, and A. J. Thomson, unpublished data).

Neither metal is observed by EPR spectroscopy, and the most likely explanation is that there is a spin-interaction between them. This implies that Fe_B, the non-heme iron of the dinuclear site, is in the ferric state making the overall center an even-electron non-Kramers system. We did not

observe the $g = 2.009$ signal reported for *P. denitrificans* NOR and assigned to a high-spin non-heme ferric ion (*37*). For a high-spin ferric ion to produce such a signal would require ideal tetrahedral or octahedral symmetry, something unprecedented in a metalloprotein. A similar feature has been observed in semi-pure preparations of *P. denitrificans* NOR and on the basis of its *g*-value and power-dependence is believed to be due to an oxidized three-iron cluster contaminant (N. J. Watmough, personal communication). Hence, the properties of the active site heme are consistent with histidine−hydroxide ligation. The substantial red-shift in the energy of the low-spin ferric NIR CT band and the spin-coupling between the two ferric ions both suggest that a hydroxide may be acting as a bridging ligand. In such a conformation it could mediate the spin coupling via an exchange mechanism and its effective ligand strength at the heme would be substantially decreased. However, it should be noted that while H_2O as a bridging ligand would not send the heme low-spin at any temperature, the properties of a μ-oxo-bridged heme/non-heme iron arrangement are not known.

This work provides further evidence in support of proposals that the active site of NOR contains a heme in spin interaction with a non-heme iron ion, the latter having replaced the Cu_B found in for the HCOs. There is only one report of NOR being able to catalyze the reduction of dioxygen, although CCO can mediate the reduction of NO only at very slow rates. The nature of the metal ion paired with the heme in the active site may be therefore crucial in determining the specificity of these enzymes.

REFERENCES

1. Zumft, W. G. (1993) *Arch. Microbiol. 160*, 253−264.
2. Hochstein, L. I., and Tomlinson, G. A. (1988) *Annu. Rev. Microbiol. 42*, 231−261.
3. Berks, B. C., Ferguson, S. J., Moir, J. W. B., and Richardson, D. J. (1995) *Biochim. Biophys. Acta 1232*, 97−173.
4. Zumft, W. G. (1997) *Microbiol. Mol. Biol. Rev. 61*, 533−616.
5. Heiss, B., Frunzke, K., and Zumft, W. G. (1989) *J. Bacteriol. 171*, 3288−3297.
6. Carr, G. J., and Ferguson, S. J. (1990) *Biochem. J. 269*, 423−429.
7. Jones, A. M., and Hollocher, T. C. (1993) *Biochim. Biophys. Acta 1144*, 359−366.
8. Zumft, W. G., Gotzmann, D. J., Frunzke, K., and Viebrock, A. (1987) Novel terminal oxidoreductases of anaerobic respiration (denitrification) from *Pseudomonas*, in *Inorganic nitrogen metabolism* (Ullrich, W. R., Aparicio, P. J., Syrett, P. J., and Castillo, F., Eds.), pp 61−67, Springer-Verlag, Berlin.
9. Averill, B. A., and Tiedje, J. M. (1982) *FEBS Lett. 138*, 8−11.
10. Garber, E. A. E., and Hollocher, T. C. (1981) *J. Biol. Chem. 256*, 5459−5465.
11. Weeg-Aerssens, E. J. M., Tiedje, J. M., and Averill, B. A. (1986) *J. Biol. Chem. 261*, 9652−9656.
12. Zumft, W. G., Döhler, K., Körner, H., Löchelt, S., Viebrock, A., and Frunzke, K. (1988) *Arch. Microbiol. 149*, 492−498.
13. Ye, R. W., Averill, B. A., and Tiedje, J. M. (1992) *J. Bacteriol. 174*, 6653-6658.
14. Braun, C., and Zumft, W. G. (1991) *J. Biol. Chem. 266*, 22785−22788.
15. Kastrau, D. H. W., Heiss, B., Kroneck, P. M. H., and Zumft, W. G. (1994) *Eur. J. Biochem. 222*, 293−303.
16. Fujiwara, T., and Fukumori, Y. (1996) *J. Bacteriol. 178*, 1866−1871.
17. Zumft, W. G., Braun, C., and Cuypers, H. (1994) *Eur. J. Biochem. 219*, 481−490.
18. van der Oost, J., de Boer, A. P. N., de Gier, J.-W. L., Zumft, W. G., Stouthamer, A. H., and van Spanning, R. J. M. (1994) *FEMS Microbiol. Lett. 121*, 1−10.
19. Saraste, M., and Castresana, J. (1994) *FEBS Lett. 341*, 1−4.
20. Arai, H., Igarashi, Y., and Kodama, T. (1995) *Biochim. Biophys. Acta 1261*, 279−284.
21. de Boer, A. P. N., van der Oost, J., Reijnders, W. N. M., Westerhoff, H. V., Stouthamer, A. H., and van Spanning, R. J. M. (1996) *Eur. J. Biochem. 242*, 592−600.
22. Trumpower, B. L., and Gennis, R. B. (1994) *Annu. Rev. Biochem. 63*, 675−716.
23. Iwata, S., Ostermeier, C., Ludwig, B., and Michel, H. (1995) *Nature 376*, 660−669.
24. Tsukihara, T., Aoyama, H., Yamashita, E., Tomizaki, T., Yamaguchi, H., Shinzawa-Itoh, K., Nakashima, R., Yaono, R., and Yoshikawa, S. (1995) *Science 269*, 1069−1074.
25. Tsukihara, T., Aoyama, H., Yamashita, E., Tomizaki, T., Yamaguchi, H., Shinzawa-Itoh, K., Nakashima, R., Yaono, R., and Yoshikawa, S. (1996) *Science 272*, 1136−1144.
26. Van Gelder, B. F., Orme-Johnson, W. H., Hansen, R. E., and Beinert, H. (1967) *Proc. Natl. Acad. Sci. U.S.A. 58*, 1073−1079.
27. Van Gelder, B. F., and Beinert, H. (1969) *Biochim. Biophys. Acta 189*, 1−24.
28. Wikstrom, M., Krab, K., and Saraste, M. (1981) in *Cytochrome Oxidase, A Synthesis*, Academic Press, London.
29. Salerno, J. C., Bolgiano, B., Poole, R. K., Gennis, R. B., and Ingledew, W. J. (1990) *J. Biol. Chem. 265*, 4364−4368.
30. Moody, A. J. (1996) *Biochim. Biophys. Acta 1276*, 6−20.
31. Hosler, J. P., Ferguson-Miller, S., Calhoun, M. W., Thomas, J. W., Hill, J., Lemieux, L., Ma, J., Georgiou, C., Fetter, J., Shapleigh, J., Tecklenburg, M. M. J., Babcock, G. T., and Gennis, R. B. (1993) *J. Bioenerg. Biomembr. 25*, 121−136.
32. García-Horsman, J. A., Berry, E., Shapleigh, J. P., Alben, J. O., and Gennis, R. B. (1994) *Biochemistry 33*, 3113−3119.
33. Preisig, O., Antamatten, D., and Hennecke, H. (1993) *Proc. Natl. Acad. Sci. U.S.A. 90*, 3309−3313.
34. Keefe, R. G., and Maier, R. J. (1993) *Biochim. Biophys. Acta 1183*, 91−104.
35. de Gier, J.-W. L., Lübben, M., Reijnders, W. N. M., Tipker, C. A., Slotboom, D.-J., van Spanning, R. J. M., Stouthamer, A. H., and van der Oost, J. (1994) *Mol. Microbiol. 13*, 183−196.
36. Gray, K. A., Grooms, M., Myllykallio, H., Moomaw, C., Slaughter, C., and Daldal, F. (1994) *Biochemistry 33*, 3120−3127.
37. Girsch, P., and de Vries, S. (1997) *Biochim. Biophys. Acta 1318*, 202−216.
38. Dermastia, M., Turk, T., and Hollocher, T. C. (1991) *J. Biol. Chem. 266*, 10899−10905.
39. Brudvig, G. W., Stevens, T. H., and Chan, S. I. (1980) *Biochemistry 19*, 5275−5285.
40. Blokzijl-Homan, M. F. J., and Van Gelder, B. F. (1971) *Biochim. Biophys. Acta 234*, 493−498.
41. Zhao, X.-J., Sampath, V., and Caughey, W. S. (1995) *Biochem. Biophys. Res. Commun. 212*, 1054−1060.
42. Wang, C.-S., and Smith, R. L. (1975) *Anal. Biochem. 63*, 414−417.
43. Gadsby, P. M. A., and Thomson, A. J. (1990) *J. Am. Chem. Soc. 112*, 5003−5011.
44. Thomson, A. J., Cheesman, M. R., and George, S. J. (1993) *Methods Enzymol. 226*, 199−232.
45. Aasa, R., and Vänngård, T. (1975) *J. Magn. Reson. 19*, 308−315.
46. Lemberg, R., and Legge, J. W. (1949) in *Hematin Compounds and Bile Pigments*, Interscience Publishers, New York.
47. Eaton, W. A., and Hochstrasser, R. M. (1967) *J. Chem. Phys. 46*, 2533−2539.
48. Cheesman, M. R., Kadir, F. H. A., Al-Basseet, J., Al-Massad, F., Farrar, J., Greenwood, C., Thomson, A. J., and Moore, G. R. (1992) *Biochem. J. 286*, 361−362.

49. McKnight, J., Cheesman, M. R., Thomson, A. J., Miles, J. S., and Munro, A. W. (1993) *Eur. J. Biochem. 213*, 683−687.
50. Cheesman, M. R., Greenwood, C., and Thomson, A. J. (1991) *Adv. Inorg. Chem. 36*, 201−255.
51. Braterman, P. S., Davies, R. C., and Williams, R. J. P. (1964) *Adv. Chem. Phys. 7*, 359−407.
52. Cheng, J. C., Osborne, G. A., Stephens, P. J., and Eaton, W. A. (1973) *Nature 241*, 193−194.
53. Cheesman, M. R., Watmough, N. J., Gennis, R. B., Greenwood, C., and Thomson, A. J. (1994) *Eur. J. Biochem. 219*, 595−602.
54. Little, R. H., Cheesman, M. R., Thomson, A. J., Greenwood, C., and Watmough, N. J. (1996) *Biochemistry 35*, 13780−13787.
55. Walker, F. A., Huynh, B. H., Scheidt, W. R., and Osvath, S. R. (1986) *J. Am. Chem. Soc. 108*, 5288−5297.
56. Griffith, J. S. (1971) *Mol. Phys. 21*, 135−139.
57. De Vries, S., and Albracht, S. P. J. (1979) *Biochim. Biophys. Acta 546*, 334−340.
58. Gadsby, P. M. A., Hartshorn, R. T., Moura, J. J. G., Sinclair-Day, J. D., Sykes, A. G., and Thomson, A. J. (1989) *Biochim. Biophys. Acta 994*, 37−46.
59. Visser, J. M., de Jong, G. A. H., de Vries, S., Robertson, L. A., and Kuenen, J. G. (1997) *FEMS Microbiol. Lett. 147*, 127−132.
60. Cheesman, M. R., Watmough, N. J., Pires, C. A., Turner, R., Brittain, T., Gennis, R. B., Greenwood, C., and Thomson, A. J. (1993) *Biochem. J. 289*, 709−718.
61. Brill, A. S., and Williams, R. J. P. (1961) *Biochem. J. 78*, 246−253.
62. Dawson, J. H., and Dooly, D. M. (1989) in *Physical Bioinorganic Chemistry Series*, *Iron Porphyrins, Part II* (Lever, A. B. P., and Gray, H. B., Eds.) Chapter 1, VCH Publishers, New York.
63. Thomson, A. J., Eglinton, D. G., Hill, B. C., and Greenwood, C. (1982) *Biochem. J. 207*, 167−170.
64. George, P., Beetlestone, J., and Griffith, J. S. (1964) *Rev. Mod. Phys. 36*, 441−463.

BI972437Y